JOURNAL OF PHYSICAL ORGANIC CHEMISTRY
*J. Phys. Org. Chem.* 2007; **20:** 19–29
Published online in Wiley InterScience
(www.interscience.wiley.com) DOI: 10.1002/poc.1119



# A computational study into the reactivity of epichlorohydrin and epibromohydrin under basic conditions in the gas phase and solution

**G. N. Merrill***

Department of Chemistry, University of Texas at San Antonio, San Antonio, Texas 78249, USA

*Received 23 August 2006; revised 18 September 2006; accepted 18 September 2006*

ABSTRACT: *Ab initio* molecular orbital calculations were carried out on epibromohydrin (EBH) and epichlorohydrin (ECH) in an attempt to elucidate their reactivity with respect to a hard nucleophile, hydroxide. These systems were modeled in both the gas phase and a polar solvent under basic conditions. In the gas phase, it was determined that a direct displacement mechanism (nucleophilic attack at the C1 position) was operative for EBH, while an indirect pathway (nucleophilic attack at the C3 position and subsequent intramolecular displacement) was followed for ECH. In an acetone solution, only the indirect displacement mechanism was found to occur. An electrostatic argument is advanced to account for this behavior in polar solution. Copyright © 2007 John Wiley & Sons, Ltd.

KEYWORDS: epibromohydrin; epichlorohydrin; hydroxide; reaction mechanism; gas phase; solution; *ab initio* modeling

## INTRODUCTION

The structure and reactivity of small ring systems continue to fascinate organic chemists.[1] The source of this fascination derives largely from the fact that these compounds offer glimpses into the extremes of bonding in carbon-containing compounds. Of particular interest are heterocycles, the epoxide moiety being one of the principal archetypes.

Epihalohydrins provide physical organic chemists with systems that permit the nucleophilic reactivity of epoxides relative to alkyl halides to be assessed. For instance, does the ring strain associated with the epoxide promote nucleophilic attack at the cyclic methylene (C3) or methine (C2) positions over that at the acyclic methylene (C1) position? If it does, can an appropriate choice of the halide or solvent alter this preference?

Epihalohydrins are commercially important compounds. For example, epichlorohydrin (ECH) is used in the industrial production of glycerol, various resins, and a variety of elastomers.[2] It has also found use in the synthesis of optically active isomers of drugs.[3] It is for these reasons, academic and industrial, that epihalohydrins have been the subject of a number of experimental investigations over the last half century.[4]

**Correspondence to:* G. N. Merrill, Department of Chemistry, University of Texas at San Antonio, 6900 North Loop 1604 West, San Antonio, TX 78249, USA.
E-mail: grant.merrill@utsa.edu

McClure *et al.*[5] examined the reactivity of 1-X-2,3-epoxy-propanes (X = Cl, MsO, and TfO) with *p*-Y-phenolates (Y = H, CN, and MeO) under a variety of reaction conditions. When ECH was allowed to react with phenolate in acetone, nucleophilic attack occurred predominantly at the C3 position (C3:C1 = 19:1). When the reaction was carried out in dimethyl formamide (DMF), however, phenolate was found to react with ECH at both the C3 and C1 positions (C3:C1 = 1:1). When the same reactions were carried out with a better leaving group (the mesylate derivative), attack at the C1 position increased (in acetone, C3:C1 = 4:1; in DMF, C3:C1 = 5.7:1). Similarly, running the reaction in methylene chloride ($CH_2Cl_2$) with the triflate derivative led exclusively to attack at the C1 position (C3:C1 = 1:49). These results suggest that solvent and leaving-group effects are important in determining the reactivity of epihalohydrins: more polar solvents and better leaving groups increase the likelihood of attack at the C1 position. Ohishi and Nakanishi[6] conducted a similar study of ECH. They reacted ECH with a phenolate (the potassium salt of 2-acetyl-7-hydroxy-benzo[*b*]furan) in DMF. They found attack was again slightly preferred at the C3 position over that at the C1 position (C3:C1 = 7:5).

The reactivity of epibromohydrin (EBH) with catecholate anion in a 1:1 solution of ethanol and water (EtOH:$H_2O$) was examined by Cawley and Onat.[7] They determined that attack at both the C1 and C3 positions occurred, with attack at the C3 position being slightly favored. They were also able to calculate enthalpies

($\Delta_{\ddagger}H$: C1 = 19 and C3 = 12 kcal mol$^{-1}$), entropies ($\Delta_{\ddagger}S$: C1 = −18 and C3 = −34 cal K$^{-1}$ mol$^{-1}$), and free energies ($\Delta_{\ddagger}G$: C1 = 24 and C3 = 22 kcal mol$^{-1}$) for the two pathways. These results highlight that the two mechanisms are governed by two very different factors: enthalpic in the case of C3 attack and entropic for C1 attack.

Whalen[8] conducted an acetolysis study of ECH. He discovered that the reaction involved little ionization at the C1 position and that attack occurred initially at the C3 position. He was also able to put forth indirect evidence that attack occurred at the C2 and the C3 positions.

A very limited number of computational investigations of epihalohydrins have appeared in the literature. Politzer and Laurence[9] reported on a study of the reactivity of ECH with ammonia in the gas phase. This work was performed at a low level of theory by current standards (partial optimizations at the Hartree-Fock level with the STO-3G basis set), and they therefore offer only qualitative insights into the reactivity and structure of ECH. A systematic study of the reactivity of ECH with hydroxide in the gas phase has been recently reported by us.[10] It was found that nucleophilic attack was preferred at the C3 position in the gas phase.

The current paper extends our earlier work into the reactivity of epihalohydrins in the gas phase and solution. The goals of this research were (1) to establish the importance of leaving-group effects (Cl vs. Br) and (2) to determine the influence of solvent upon the reactivity of epihalohydrins. In the course of this research, detailed gas-phase and solution reaction coordinates were established. While these results should be of general interest to physical organic chemists, they should also be of particular relevance to synthetic organic chemists in carrying out reactions involving epihalohydrins and related systems.

## COMPUTATIONAL METHODS

The following computational procedure was employed in carrying out the current calculations.

1. Structures were fully optimized at the restricted Hartree-Fock (RHF)[11] level of theory with the double split-valence 6-31G basis set[12] to which sets of d-polarization[13] and sp-diffuse[14] functions were added to all atoms save hydrogen; that is, the 6-31+G(d) basis set. Structures were held to be converged when the maximum and root-mean-square of the gradients fell below 0.012 and 0.004 kcal mol$^{-1}$ Å$^{-1}$, respectively (1 kcal = 4.184 kJ and 1 Å = 10$^{-10}$ m). All relevant stationary points were located and fully characterized.
2. Hessian matrices were computed for all stationary points (minima and transition states) at the same level as used for the optimizations. The absence of negative eigenvalues confirmed a stationary point as a minimum, while the presence of a single negative eigenvalue established the stationary point as a transition state.
3. Enthalpic and entropic corrections were calculated for all stationary points using standard statistical mechanical formulae.[15] All vibrational frequencies were scaled by an empirical factor of 0.8953 to compensate for the known overestimation of these values by the harmonic approximation at the RHF level with double-zeta quality bases.[16] Thermodynamic corrections were made to 1 atm and 298 K.
4. To verify that all transition states corresponded to the appropriate minima, intrinsic reaction coordinate (IRC)[17] calculations were performed. These calculations established the minimum energy path (MEP) between all *reactants* and *products*.
5. As many of the transition states involved bond formation and breaking, electron correlation effects were predicted to be important. Single-point energy calculations were therefore carried out on the optimized structures. These calculations were performed at the second-order perturbation (MP2),[18] density functional (B3LYP),[19] and couple-clustered (CCSD)[20] levels of theory using the 6-31+G(d) basis. Single-point energies were also computed at the MP2 and B3LYP levels with the aug-cc-pVDZ[21] basis. Only valence electrons were correlated in the MP2 calculations; that is, the frozen-core (fc) approximation[22] was employed.
6. Solvation effects were calculated with the integral equation formalism of the polarizable continuum model (IEF-PCM)[23] by computing RHF single-point energies with the 6-31+G(d) basis. Cavitation energies were computed via the method of Pierotti and Claverie,[24] while repulsion and dispersion energies were determined by the procedure of Amovilli and Mennucci.[25] Solute electron charge density that escaped from the solvent cavity was explicitly treated by the method of Mennucci and Tomasi.[26] Acetone ($CH_3COCH_3$) was selected as a representative polar, aprotic solvent.

All calculations were performed with the GAMESS program[27] on a small Beowulf cluster of personal computers.

## RESULTS AND DISCUSSION

The reactivity of hydroxide ($OH^-$) with ECH and EBH was examined in the gas phase and solution. The gas-phase reactivity represents the intrinsic behavior of epihalohydrins with respect to (hard) nucleophiles given that it is free of solvent, counterion, and aggregation effects. The gas-phase results also serve as a point of departure for treating the systems in condensed media.



DOI: 10.1002/poc

Unless otherwise noted, the following results pertain to energies, etc., determined at the MP2/aug-cc-pVDZ level of theory for HF/6-31+G(d) optimized geometries and Hessians. Results obtained at the HF/aug-cc-pVDZ level will be mentioned where they differ significantly from those found at the MP2/aug-cc-pVDZ level.

## Gas-phase pathways

The lowest energy conformers for the epihalohydrins have anti conformations, while the two gauche conformers are only marginally higher in energy [refer to Figs 1–3 in Reference 10 for those structures not explicitly discussed]. Here, *anti* and *gauche* are defined for the halogen atom with respect to the oxygen atom of the epoxide ring. These three conformers interact with hydroxide to form a variety of ion–molecule complexes (Fig. 1). The lowest energy reactant ion–molecule complex (RIM) results from a charge–dipole interaction between hydroxide and the gauche(-) conformer for the epihalohydrins. The formation of these complexes is significantly exothermic ($\Delta$H: RIM(Cl) = −23.8; RIM(Br) = −23.3 kcal mol$^{-1}$) and exergonic ($\Delta$G: RIM(Cl) = −16.4; RIM(Br) = −16.2 kcal mol$^{-1}$). This decrease in energy provides the driving force behind the subsequent displacement reactions.

The central goal in the study was to determine where nucleophilic attack by hydroxide, an archetypal (hard) nucleophile under basic conditions, takes place in the epihalohydrins: the acyclic methylene (C1), cyclic methine (C2), or cyclic methylene (C3) position. Two transition states (TS) were located for attack at the C1 position of the epihalohydrins, corresponding to the two gauche conformers; repeated attempts to find an analogous anti-TS were unsuccessful. The lowest energy transition states were found for the gauche(-) conformers (TS1 in Fig. 2). Both transition states possessed *negative* activation energies (i.e., the transition states were lower in energy than the separated reactants) with the bromo TS being favored by about 2.5 kcal mol$^{-1}$ ($\Delta$H: TS1(Cl) = −15.0; TS1(Br) = −17.5; $\Delta$G: TS1(Cl) = −6.3; TS1(Br) = −8.8 kcal mol$^{-1}$). Clearly, entropic effects are important in reducing the absolute magnitude of the activation energies, but they do not affect the relative values to any real degree. These results are consistent with bromide being a better leaving group than chloride. An examination of the C1—X bond lengths (Fig. 2) reveals that the transition state for EBH occurs earlier than that for ECH; the C1—Br bond is only 19% elongated over that in EBH, while the C1—Cl bond is 69% longer than that in ECH.

Subsequent to this transition state, a product ion–molecule complex (PIM1) is formed between glycidol and the halide (Fig. 1). The complex is the result of hydrogen bond formation between the hydroxyl group and the halide, and its formation is appreciably exothermic ($\Delta$H: PIM1(Cl) = −69.7; PIM1(Br) = −73.5 kcal mol$^{-1}$) and exergonic ($\Delta$G: PIM1(Cl) = −61.5; PIM1(Br) = −65.7 kcal mol$^{-1}$).

The reaction is overall exothermic ($\Delta_r$H: ECH + OH$^-$ = −50.3; EBH + OH$^-$ = −56.0 kcal mol$^{-1}$) and exergonic ($\Delta_r$G: ECH + OH$^-$ = −48.2; EBH + OH$^-$ = −54.0 kcal mol$^{-1}$), with the bromo pathway being almost 6 kcal mol$^{-1}$ more exothermic/exergonic. This result is consistent with the lower activation energy along the bromo pathway for the rate-limiting step. The complete energetics for the direct displacement mechanism (Pathway 1 in Fig. 3) are given in Table 1.

Nucleophilic attack can also occur at the methylene position of the epoxide ring (C3). The activation energy for this pathway is also negative (Pathway 2 in Fig. 1). For attack on ECH, the activation energies are actually less for attack at the C3 position ($\Delta$H = −16.6; $\Delta$G = −7.9 kcal mol$^{-1}$) than the C1 position. This is not the case for attack on EBH, where attack on the C3 position is less favored ($\Delta$H = −16.9; $\Delta$G = −8.2 kcal mol$^{-1}$). These results suggest the two epihalohydrins have intrinsically different reactivities. In both transition states, the C3—O bond is stretched 25% over that found in the respective epihalohydrin (TS2a in Fig. 2). The TS2a transition state occurs earlier than that for the TS1 transition state in ECH, but it occurs later for EBH. It is also worth noting that, excluding the C1—X bond, the two TS2a transition states are virtually identical; for example, C3—O = 1.75 Å. This indicates that the halide and epoxide ring are effectively insulated from molecular orbital interactions by the C1 methylene group.

Following attack at the C3 position, ring opening occurs, and a stable alkoxy intermediate is formed (INT1). The formation of this intermediate is significantly exothermic ($\Delta$H: INT1(Cl) = −59.8; INT1(Br) = −60.6 kcal mol$^{-1}$) and exergonic ($\Delta$G: INT1(Cl) = −49.7; INT1(Br) = −50.7 kcal mol$^{-1}$). Product (glycidol) formation can take place from the intramolecular attack of the C2 methine oxygen atom on the C1 methylene carbon atom; that is, the epoxide is reformed with loss of the halide. The enthalpy of activation for this step is far less than that for the initial attack on the epoxide ring ($\Delta$H: TS2b(Cl) = −51.7; TS2b(Br) = −55.4 kcal mol$^{-1}$); the free energy of activation is also more favorable ($\Delta$G: TS2b(Cl) = −41.8; TS2b(Br) = −45.6 kcal mol$^{-1}$). Ring opening by hydroxide is therefore predicted to be quickly followed by reformation of a new epoxide ring with loss of the halide. This leads to PIM1 and finally the products (glycidol and halide). The energetics associated with the indirect displacement mechanism (Pathway 2 in Fig. 3) are given in Table 2.

Nucleophilic attack could also occur in principle at the methine position of the epoxide ring (C2), so the transition states for this pathway (Pathway 3 in Fig. 1) were also located. These activation energies prove to be less favorable than those for attack at either the C1 or C3



DOI: 10.1002/poc

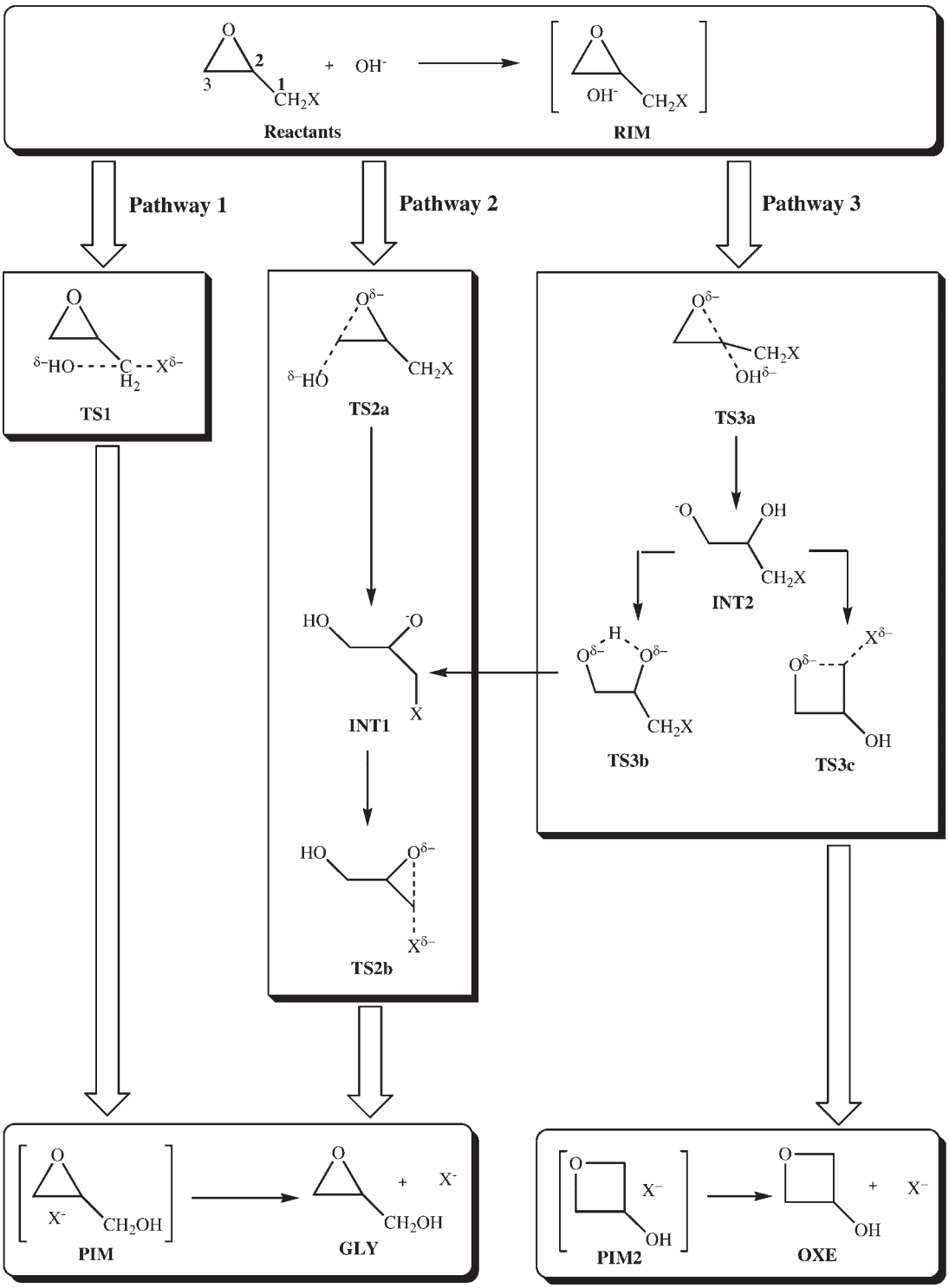


**Figure 1.** Mechanistic pathways for nucleophilic attack by hydroxide on epihalohydrins.

positions ($\Delta$H: TS3a(Cl) = −13.5; TS3a(Br) = −13.8; $\Delta$G: TS3a(Cl) = −4.6; TS3a(Br) = −5.1 kcal mol$^{-1}$). It is therefore predicted that this pathway is not operative to any great extent for either epihalohydrin. Again, the two transition states are essentially identical, with both occurring slightly later than those for nucleophilic attack at the C3 position (TS3a in Fig. 2).

Attack by hydroxide at the C2 position also leads to ring opening and subsequent formation of an alkoxy intermediate (INT2). While this intermediate is predicted



DOI: 10.1002/poc

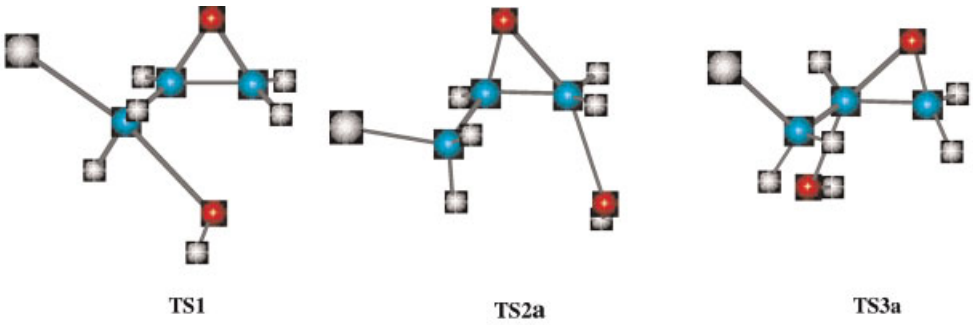


| Distance | TS1 | | TS2a | | TS3a | |
|---|---|---|---|---|---|---|
| | ECH | EBH | ECH | EBH | ECH | EBH |
| C1-X | 2.21 (+69%) | 2.33 (+19%) | 1.83 (+2%) | 1.98 (+2%) | 1.82 (+2%) | 1.98 (+2%) |
| C1-C2 | 1.49 (-1%) | 1.49 (-1%) | 1.51 (+1%) | 1.51 (+1%) | 1.50 (0%) | 1.49 (-1%) |
| C2-C3 | 1.45 (-1%) | 1.45 (-1%) | 1.44 (-1%) | 1.44 (-1%) | 1.44 (-1%) | 1.44 (-1%) |
| C2-O | 1.41 (+1%) | 1.41 (+1%) | 1.37 (0%) | 1.37 (-2%) | 1.80 (+29%) | 1.79 (+28%) |
| C3-O | 1.41 (+1%) | 1.41 (+1%) | 1.75 (+25%) | 1.75 (+25%) | 1.37 (-2%) | 1.37 (-2%) |

**Figure 2.** Transition states for nucleophilic attack on epibromohydrin (EBH) and epichlorohydrin (ECH) by hydroxide. Structures optimized at the HF/6-31+G(d) level of theory. Percentage changes relative to respective epihalohydrin given in parentheses. All bond distances in Å.

to be stable at the HF/6-31+G(d) level of theory, it is calculated to be higher in energy than the barrier to proton transfer (TS3b) to form the more stable intermediate (INT1); that is, the process is barrierless and is most likely an artifact of the optimizations performed at the Hartree-Fock level of theory. Nucleophilic attack at the C2 position of the epihalohydrins is likely to lead to rapid interconversion of the resulting alkoxy *intermediates* with subsequent reformation of the epoxide ring via an intramolecular displacement.

It should be noted that a transition state for oxetane formation (TS3c) was also located. While these transitions states possessed activation energies much less than those for nucleophilic attack at the C2 position ($\Delta H$: TS3b(Cl) = −38.5; TS3b(Br) = −40.6; $\Delta G$: TS3b(Cl) = −28.2; TS3b(Br) = −30.4 kcal mol$^{-1}$), they are nevertheless greater in energy than those for proton transfer. Formation of 2-hydroxy oxetane (OXE) is therefore not predicted to be a major product.

The complete energetics for the mechanisms involving nucleophilic attack at the C2 position of the epihalohydrins (Pathway 3 in Fig. 3) are given in Table 3.

The gas-phase results may be summarized succinctly: nucleophilic attack is most likely to occur at the C3 (cyclic methylene) position for ECH [Eqn (1a)], while nucleophilic attack is slightly more favorable at the C1 (acyclic methylene) position for EBH [Eqn (1b)].

$$\Delta\Delta G(\mathrm{ECH} + \mathrm{OH}^-) : 0.0(\mathrm{C3}) < 1.6(\mathrm{C1}) < 3.3(\mathrm{C2})\ \mathrm{kcal\ mol}^{-1} \quad (1a)$$

$$\Delta\Delta G(\mathrm{EBH} + \mathrm{OH}^-) : 0.0(\mathrm{C1}) < 0.6(\mathrm{C3}) < 3.1(\mathrm{C2})\ \mathrm{kcal\ mol}^{-1} \quad (1b)$$

Furthermore, nucleophilic attack is least likely at the C2 (cyclic methine) positions for both epihalohydrins; even if attack were to take place at this position, rapid interconversion of the resulting alkoxy intermediate would preclude formation of an oxetane product.



DOI: 10.1002/poc

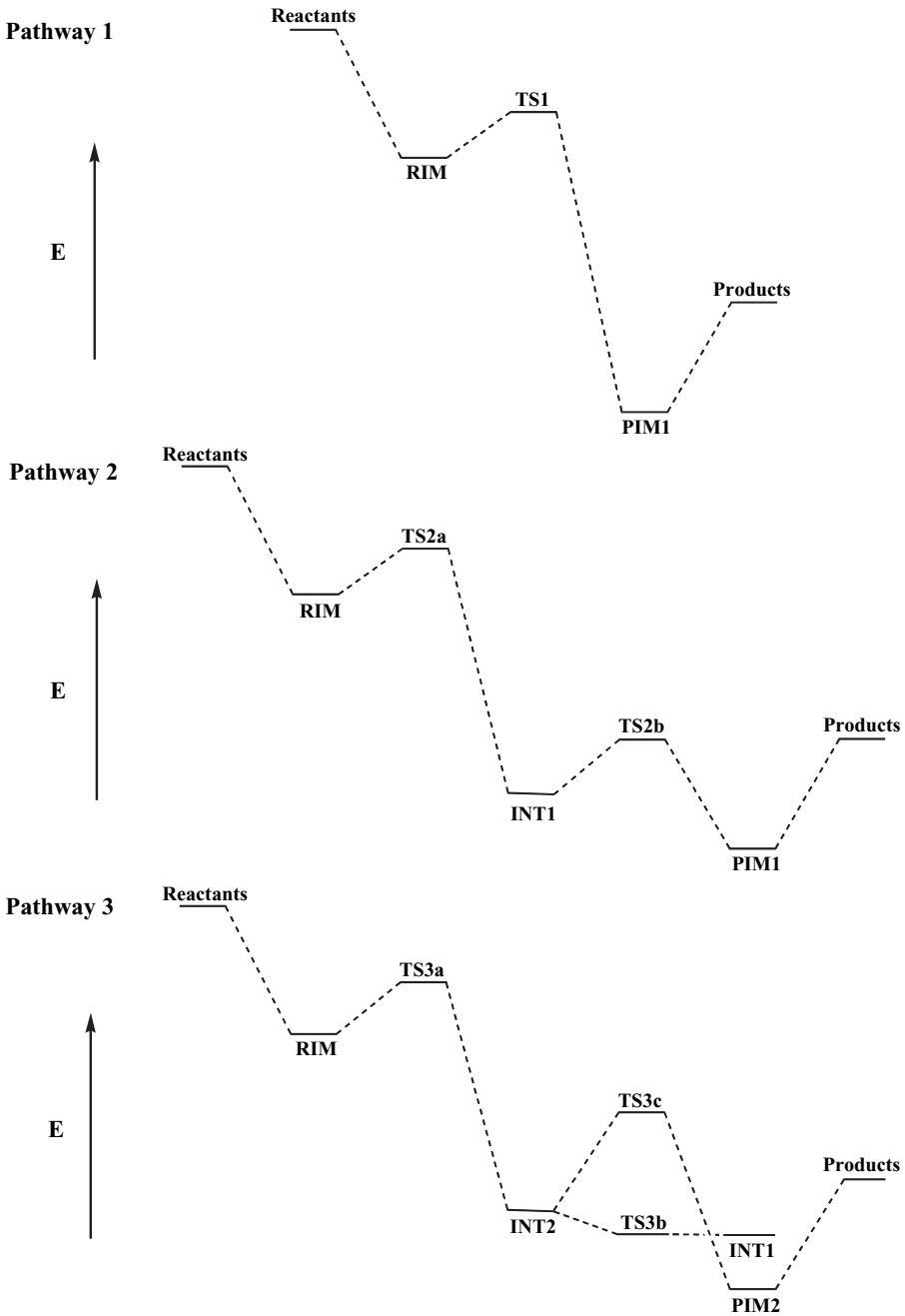


**Figure 3.** Reaction coordinates for three pathways illustrated in Fig. 1. Refer to Tables 1–3 for enthalpies and free energies.

**Table 1.** Gas-phase reaction coordinate energies for nucleophilic attack by hydroxide at the acyclic methylene (C1) position of the epihalohydrins (Pathway 1 in Fig. 1).

| Halogen | Reactants | Ion–molecule (RIM) | Transition state (TS1) | Ion–molecule (PIM1) | Products |
|---|---|---|---|---|---|
| | | | Enthalpy ΔH | | |
| Cl | 0.0 | −23.8 | −15.0 | −69.7 | −50.3 |
| Br | 0.0 | −23.2 | −17.5 | −73.5 | −56.0 |
| | | | Free energy ΔG | | |
| Cl | 0.0 (0.0) | −16.4 (7.7) | −6.3 (25.0) | −61.5 (−27.5) | −48.2 (−28.9) |
| Br | 0.0 (0.0) | −16.2 (10.3) | −8.8 (23.1) | −65.7 (−27.6) | −54.0 (−29.9) |

Parenthetical values are acetone solvated. Enthalpies (ΔH) and free energies (ΔG) in kcal mol$^{-1}$. Level of theory: MP2/aug-cc-pVDZ//HF/6-31+G(d).



DOI: 10.1002/poc

**Table 2.** Gas-phase reaction coordinate energies for nucleophilic attack by hydroxide at the cyclic methylene (C3) position of the epihalohydrins (Pathway 2 in Fig. 1).

| Halogen | Reactants | Ion–molecule (RIM) | Transition state (TS2a) | Intermediate (INT1) | Transition state (TS2b) | Ion–molecule (PIM1) | Products |
|---|---|---|---|---|---|---|---|
| | | | | Enthalpy ΔH | | | |
| Cl | 0.0 | −23.8 | −16.6 | −59.8 | −51.7 | −69.7 | −50.3 |
| Br | 0.0 | −23.2 | −16.8 | −60.6 | −55.4 | −73.5 | −56.0 |
| | | | | Free energy ΔG | | | |
| Cl | 0.0 (0.0) | −16.4 (7.7) | −7.9 (21.9) | −49.7 (−16.5) | −41.8 (−5.0) | −61.5 (−27.5) | −48.2 (−28.9) |
| Br | 0.0 (0.0) | −16.2 (10.3) | −8.2 (20.0) | −50.7 (−17.5) | −45.6 (−7.3) | −65.7 (−27.6) | −54.0 (−29.9) |

Parenthetical values are acetone solvated. Enthalpies (ΔH) and free energies (ΔG) in kcal mol$^{-1}$. Level of theory: MP2/aug-cc-pVDZ//HF/6-31+G(d).

**Table 3.** Gas-phase reaction coordinate energies for nucleophilic attack by hyrdoxide at the cyclic methine (C2) position of the epihalohydrin (Pathway 3 in Fig. 1).

| Halogen | Reactants | Ion–molecule (RIM) | Transition state (TS3a) | Intermediate (INT2) | Transition state (TS3b) | Intermediate (INT1) |
|---|---|---|---|---|---|---|
| | | | ΔH (Proton transfer) | | | |
| Cl | 0.0 | −23.8 | −13.5 | −55.5 | −59.5 | −59.8 |
| Br | 0.0 | −23.2 | −13.8 | −55.8 | −60.0 | −60.6 |
| | | | ΔG (Proton transfer) | | | |
| Cl | 0.0 (0.0) | −16.4 (7.7) | −4.6 (25.1) | −45.4 (−13.1) | −49.1 (−17.6) | −49.7 (−16.5) |
| Br | 0.0 (0.0) | −16.2 (10.3) | −5.1 (24.2) | −45.7 (−15.3) | −49.7 (−18.1) | −50.7 (−17.5) |

| Halogen | Reactants | Ion–molecule (RIM) | Transition state (TS3a) | Intermediate (INT2) | Transition state (TS3c) | Ion–molecule (PIM2) | Products |
|---|---|---|---|---|---|---|---|
| | | | | ΔH (Formation of 2-hydroxy oxetane) | | | |
| Cl | 0.0 | −23.8 | −13.5 | −55.5 | −38.5 | −70.9 | −49.6 |
| Br | 0.0 | −23.2 | −13.8 | −55.8 | −40.6 | −74.7 | −55.3 |
| | | | | ΔG (Formation of 2-hydroxy oxetane) | | | |
| Cl | 0.0 (0.0) | −16.4 (7.7) | −4.6 (25.1) | −45.4 (−13.1) | −28.2 (5.7) | −62.8 (−29.4) | −47.3 (−29.3) |
| Br | 0.0 (0.0) | −16.2 (10.3) | −5.1 (24.2) | −45.7 (−15.3) | −30.4 (13.6) | −66.3 (−28.4) | −53.1 (−30.3) |

Parenthetical values are acetone solvated. Enthalpies (ΔH) and free energies (ΔG) in kcal mol$^{-1}$. Level of theory: MP2/aug-cc-pVDZ//HF/6-31+G(d).

It should be noted that the HF/aug-cc-pVDZ results are not in agreement with the MP2/aug-cc-pVDZ results. Specifically, the HF calculations predict the following relative ordering of transitions states for ECH [Eqn (2a)] and EBH [Eqn (2b)].

$$\Delta\Delta G(\mathrm{ECH} + \mathrm{OH}^-) : 0.0(\mathrm{C1}) < 6.4(\mathrm{C3}) < 11.5(\mathrm{C2})\ \mathrm{kcal\ mol}^{-1} \quad (2a)$$

$$\Delta\Delta G(\mathrm{EBH} + \mathrm{OH}^-) : 0.0(\mathrm{C1}) < 9.6(\mathrm{C3}) < 14.6(\mathrm{C2})\ \mathrm{kcal\ mol}^{-1} \quad (2b)$$

These results would appear to indicate that nucleophilic attack should only occur at the acyclic methylene (C1) position and that there should be little competition between this mechanism and that for attack at the cyclic methylene (C3) position.

To investigate this discrepancy, additional single-point energy calculations using density functional (B3LYP) and coupled-cluster (CCSD) theory were carried out on the HF/6-31+G(d) optimized structures and Hessians. These results are collected in Table 4.

Calculations performed at the highest level of theory, CCSD/6-31+G(d)//HF/6-31+G(d), agree with those performed at the MP2 level of theory for ECH; that is, ΔΔG: C3 < C1 < C2. Specifically, the CCSD calculations lead to a 1.3 kcal mol$^{-1}$ stabilization of the TS1, a 1.8 kcal mol$^{-1}$ destabilization of the TS2a, and a 2.0 kcal mol$^{-1}$ destabilization of the TS3a with respect to the MP2 transition states. The B3LYP results support those determined at the HF level for ECH; that is, ΔΔG: C1 < C3 < C2. It should also be noted that the B3LYP activation energies are substantially lower than those found at the other three levels of theory. This *underestimation* of activation energies by density functional methods appears to be one of its characteristics.[28]

All four levels of theory agree with regards to the relative ordering of TS energies for the EBH systems; that is, ΔΔG: C1 < C3 < C2. Again, the CCSD and MP2



DOI: 10.1002/poc

**Table 4.** Comparison of enthalpies and free energies of activation as a function of level of theory.

| | TS1 | | TS2a | | TS2b | | TS3a | | TS3b | | TS3c | |
|---|---|---|---|---|---|---|---|---|---|---|---|---|
| Level/Basis | ΔH | ΔG | ΔH | ΔG | ΔH | ΔG | ΔH | ΔG | ΔH | ΔG | ΔH | ΔG |
| Epichlorohydrin: ΔΔH/G = ΔH/G(TS) − ΔH/G(reactants) | | | | | | | | | | | | |
| HF/1 | −13.7 | −4.9 | −7.1 | +1.6 | −53.9 | −43.9 | −1.9 | +7.0 | −53.9 | −43.5 | −42.1 | −31.8 |
| HF/2 | −12.6 | −3.9 | −6.2 | +2.5 | −52.3 | −42.3 | −1.4 | +7.6 | −52.8 | −42.4 | −41.1 | −30.9 |
| MP2/1 | −12.6 | −3.9 | −15.5 | −6.8 | −50.2 | −40.2 | −12.1 | −3.1 | −58.1 | −47.7 | −35.2 | −24.9 |
| MP2/2 | −15.0 | −6.3 | −16.6 | −7.9 | −51.7 | −41.8 | −13.5 | −4.6 | −59.5 | −49.1 | −38.5 | −28.2 |
| B3LYP/1 | −20.6 | −11.9 | −17.4 | −8.7 | −57.9 | −48.0 | −14.1 | −5.2 | −59.8 | −49.5 | −44.7 | −34.4 |
| B3LYP/2 | −19.1 | −10.4 | −16.1 | −7.4 | −55.0 | −45.0 | −13.0 | −4.1 | −57.7 | −47.3 | −42.7 | −32.4 |
| CCSD/1 | −13.3 | −4.6 | −13.6 | −5.0 | −51.2 | −41.3 | −10.0 | −1.1 | −57.1 | −46.8 | −37.9 | −27.7 |
| Epibromohydrin: ΔΔH/G = ΔH/G(TS) − ΔH/G(reactants) | | | | | | | | | | | | |
| HF/1 | −16.3 | −7.7 | −7.4 | +1.2 | −57.5 | −47.7 | −2.3 | +6.3 | −54.8 | −44.5 | −44.3 | −34.2 |
| HF/2 | −16.6 | −7.9 | −6.9 | +1.7 | −57.4 | −47.6 | −1.9 | +6.7 | −53.6 | −43.3 | −44.6 | −34.5 |
| MP2/1 | −16.8 | −8.2 | −15.9 | −7.3 | −55.9 | −46.1 | −12.7 | −4.0 | −59.3 | −49.1 | −39.1 | −29.0 |
| MP2/2 | −17.5 | −8.8 | −16.8 | −8.2 | −55.4 | −45.6 | −13.8 | −5.1 | −60.0 | −49.7 | −40.6 | −30.4 |
| B3LYP/1 | −22.3 | −13.6 | −17.4 | −8.8 | −60.5 | −50.6 | −14.2 | −5.5 | −60.7 | −50.4 | −46.0 | −35.8 |
| B3LYP/2 | −22.2 | −13.6 | −16.4 | −7.8 | −59.2 | −49.3 | −13.2 | −4.5 | −58.5 | −48.2 | −45.3 | −35.2 |
| CCSD/1 | −17.3 | −8.7 | −14.0 | −5.4 | −56.8 | −46.9 | −10.6 | −1.9 | −58.3 | −48.1 | −41.7 | −31.6 |

Basis 1 = 6-31+G(d); Basis 2 = aug-cc-pVDZ; TS1 = C1 attack; TS2a = C3 attack; TS2b = epoxide reformation; TS3a = C2 attack; TS3b = $H^+$ transfer; TS3c = oxetane formation. All values in kcal $mol^{-1}$.

results are in fairly close agreement with one another; the CCSD calculations lead to a 0.5 kcal $mol^{-1}$ stabilization of the TS1, a 1.9 kcal $mol^{-1}$ destabilization of the TS2a, and a 2.1 kcal $mol^{-1}$ destabilization of the TS3a *vis à vis* the MP2 transition states. The B3LYP calculations also predict the lowest absolute energies of activation.

Based upon the coupled-cluster results and the strong dependence of the density functional method on the Hartree-Fock formalism, it is probably safe to conclude that the perturbation results represent the intrinsic reactivity of the epihalohydrins in the gas phase [Eqns (1a) and (1b)].

## Solvated pathways

The polarizable continuum model (PCM) was used to investigate the effects of solvent upon the gas-phase reaction coordinate. To this end, single-point energy calculations were carried out at the HF/6-31+G(d) level upon the optimized gas-phase structures. From these calculations, the total solvent effect (TOT) was computed; it is the sum of a number of energies: wavefunction reorganization (ΔE), electrostatic (ES), cavitation (CAV), dispersion (DIS), and repulsion (REP). These energies are collected in Table 5 for acetone ($CH_3COCH_3$). This solvent was chosen as being representative of polar, aprotic solvents in general and was one of the solvents used in the experimental studies of McClure *et al.*[5]

A number of generalizations can be drawn from the PCM results. (1) The reorganization, cavitation, and repulsion energies were all positive and therefore destabilizing influences on the gas-phase reaction coordinates. Conversely, electrostatic and dispersion energies were all negative and thus stabilizing. (2) Electrostatic interactions were clearly the most important as would be expected for charged and/or dipolar species in polar solvents. The electrostatic energies also showed the greatest variation between the species (−51.8 to −97.1 kcal $mol^{-1}$, a range of nearly 40 kcal $mol^{-1}$). (3) Cavitation and dispersion effects were of next importance, averaging about 13 and −13 kcal $mol^{-1}$, respectively, and therefore nearly cancelled one another. (4) Reorganization and repulsion energies showed little variation among the species considered, averaging approximately 2 and 6 kcal $mol^{-1}$, respectively. These two destabilizing effects therefore served to mitigate the stabilization incurred from the electrostatic interactions. From the foregoing, it can be concluded that, in evaluating relative energies for similar systems or processes, only electrostatic effects need to be considered; the other energy terms would appear only to be important in computing absolute energies.

Solvation has a pronounced effect upon the gas-phase potential energy surfaces. It results chiefly in eliminating the minima associated with the reactant (RIM) and product (PIM1 and PIM2) ion–molecule complexes; that is, they are no longer stable minima along the reaction coordinates. More importantly, all three transition states corresponding to nucleophilic attack (TS1, TS2a, and TS3) now possess *positive* energies of activation (i.e., the energy of the transitions states are greater than that of the separated reactants). The transition states for intramolecular displacement of the halide to reform the epoxide ring (TS2b) still have *negative* activation energies, albeit much higher in energy than their gas-phase counterparts.



DOI: 10.1002/poc

**Table 5.** Solvation energies calculated at the HF/6-31+G(d) level of theory with the polarizable contiuum model (PCM) for acetone (kcal mol$^{-1}$).

| | Epichlorohydrin | | | | | | |
|---|---|---|---|---|---|---|---|
| | ΔE | ES | CAV | DIS | REP | TOT | ΔTOT |
| Scheme 1 | | | | | | | |
| ECH + $OH^-$ | 2.3 | −97.1 | 13.9 | −13.6 | 6.7 | −87.8 | 0.00 |
| Ion–Molecule (RIM) | 3.1 | −73.1 | 12.9 | −12.4 | 5.8 | −63.7 | 24.1 |
| Transition State (TS1) | 2.0 | −65.0 | 12.9 | −12.2 | 5.8 | −56.5 | 31.3 |
| Ion–Molecule (PIM1) | 1.9 | −62.5 | 13.3 | −11.9 | 5.4 | −53.8 | 34.0 |
| GLY + $Cl^-$ | 1.9 | −78.3 | 13.8 | −12.3 | 6.4 | −68.5 | 19.3 |
| Scheme 2 | | | | | | | |
| Transition State (TS2a) | 2.2 | −66.5 | 13.0 | −12.3 | 5.6 | −58.0 | 29.8 |
| Intermediate (INT1) | 2.5 | −62.6 | 12.3 | −12.0 | 5.2 | −54.6 | 33.2 |
| Transition State (TS2b) | 1.5 | −58.4 | 12.7 | −12.1 | 5.3 | −51.0 | 36.8 |
| Scheme 3 | | | | | | | |
| Transition State (TS3a) | 2.3 | −66.5 | 12.8 | −12.2 | 5.5 | −58.1 | 29.7 |
| Intermediate (INT2) | 2.5 | −63.5 | 12.3 | −12.0 | 5.2 | −55.5 | 32.3 |
| Transition State (TS3b) | 2.5 | −63.7 | 12.1 | −12.2 | 5.0 | −56.3 | 31.5 |
| Transition State (TS3c) | 2.1 | −61.5 | 12.3 | −12.2 | 5.4 | −53.9 | 33.9 |
| Ion–Molecule (PIM2) | 1.9 | −62.9 | 12.9 | −12.0 | 5.7 | −54.4 | 33.4 |
| OXE + $Cl^-$ | 1.9 | −79.5 | 13.6 | −12.3 | 6.5 | −69.8 | 18.0 |
| | Epibromohydrin | | | | | | |
| | ΔE | ES | CAV | DIS | REP | TOT | ΔTOT |
| Scheme 1 | | | | | | | |
| EBH + $OH^-$ | 2.3 | −97.0 | 14.3 | −14.0 | 6.8 | −87.6 | 0.0 |
| Ion–Molecule (RIM) | 3.0 | −74.0 | 13.4 | −12.5 | 6.0 | −64.1 | 23.5 |
| Transition State (TS1) | 2.2 | −64.4 | 13.2 | −12.7 | 6.0 | −55.7 | 31.9 |
| Ion–Molecule (PIM1) | 1.7 | −58.1 | 13.8 | −12.5 | 5.6 | −49.5 | 38.1 |
| Scheme 2 | | | | | | | |
| GLY + $Br^-$ | 2.2 | −73.2 | 14.2 | −13.3 | 6.6 | −63.5 | 24.1 |
| Transition State (TS2a) | 2.6 | −68.3 | 13.4 | −12.9 | 5.8 | −59.4 | 28.2 |
| Intermediate (INT1) | 3.0 | −62.8 | 12.6 | −12.5 | 5.3 | −54.4 | 33.2 |
| Transition State (TS2b) | 1.6 | −56.6 | 13.0 | −12.7 | 5.4 | −49.3 | 38.3 |
| Scheme 3 | | | | | | | |
| Transition State (TS3a) | 2.5 | −66.8 | 13.1 | −12.7 | 5.6 | −58.3 | 29.3 |
| Intermediate (INT2) | 3.4 | −66.1 | 12.7 | −12.6 | 5.4 | −57.2 | 30.4 |
| Transition State (TS3b) | 3.0 | −63.9 | 12.4 | −12.7 | 5.2 | −56.0 | 31.6 |
| Transition State (TS3c) | 2.7 | −51.8 | 12.6 | −12.8 | 5.7 | −43.6 | 44.0 |
| Ion–Molecule (PIM2) | 1.7 | −58.0 | 13.4 | −12.6 | 5.8 | −49.7 | 37.9 |
| OXE + $Br^-$ | 2.2 | −74.4 | 14.0 | −13.3 | 6.7 | −64.8 | 22.8 |

See text for computational details.

The transition states for intramolecular proton transfer (TS3b) behave in a similar fashion. Finally, the transition states for intramolecular displacement of the halide to form the oxetane ring (TS3c) are now found to possess positive energies of activation.

In an acetone solution, nucleophilic attack by hydroxide on ECH is still predicted to be favored at the cyclic methylene (C3) position; an activation free energy of 21.9 kcal mol$^{-1}$ was computed. Nucleophilic attack at the other two carbon sites was found to have similar free energies of activation: acyclic methylene (C1) = 25.0, cyclic methine (C2) = 25.1 kcal mol$^{-1}$. These theoretical results are consistent with the experimental observations of McClure *et al*.[5] The reactivity of ECH toward hard nucleophiles in polar, aprotic solvents is therefore expected to mirror that found in the gas phase with attack at the C1 position being slightly less favorable [Eqn (3a)].

$$\Delta\Delta G(\mathrm{ECH} + \mathrm{OH}^-) : 0.0(\mathrm{C3}) < 3.1(\mathrm{C1}) < 3.2(\mathrm{C2})\ \mathrm{kcal\ mol}^{-1} \quad (3a)$$

For EBH in acetone solution, one finds that nucleophilic attack by hydroxide is also favored at the C3 position, followed by attack at the C1 and C2 positions; here activation free energies of 20.0, 23.1, and 24.2 kcal mol$^{-1}$, respectively, were calculated. The values for attack at the C3 and C1 positions agree fairly well with those found experimentally by Cawley and Onat:[7]



DOI: 10.1002/poc

**Table 6.** Dipole moments calculated at the MP2/aug-cc-pVDZ//HF/6-31+G(d) level of theory for the transition states corresponding to nucleophilic attack by hydroxide on epibromohydrin (EBH) and epichlorohydrin (ECH).

| | Dipole moment (D) | |
|---|---|---|
| Transition state | EBH | ECH |
| TS1 (C1 position: acyclic methylene) | 4.04 (gas) | 2.66 |
| TS2a (C3 position: cyclic methylene) | 7.55 (sol) | 4.60 (gas and sol) |
| TS3a (C2 position: cyclic methine) | 4.46 | 2.16 |

Transition states with the lowest free energies of activation are parenthetically noted: gas phase = gas; solution = sol.

$\Delta G(C3) = 22$; $\Delta G(C1) = 24\,\text{kcal mol}^{-1}$. This leads to a relative ordering of transition state energies [Eqn (3b)] that differs from that found in the gas phase.

$$\Delta\Delta G(\text{EBH} + \text{OH}^-) : 0.0(\text{C3}) < 3.1(\text{C1}) < 4.2(\text{C2})\ \text{kcal mol}^{-1} \quad (3b)$$

That is to say, attack is now more favored at the C3 position. Polar aprotic solvents therefore appear to lower the activation energies of the transition states associated with ring opening relative to attack at the acyclic position. This general conclusion is also consistent with experiment.[5–7]

The solution results can be readily rationalized by examining the electrostatics associated with the three transition states to nucleophilic attack. In the gas phase, a sizable dipole moment ($\mu = 7.55$ D) develops for the transition state corresponding to attack on the C3 position of EBH. This dipole is 3.51 D larger than that found for the transition state to attack at the C1 position (Table 6). As electrostatic effects are dominant in the polar solvent acetone, the dipole associated with TS2a is stabilized to a greater extent than that of TS1. The difference in the respective electrostatic energies, $\Delta ES = ES(TS2a) - ES(TS1)$, is $-3.9\,\text{kcal mol}^{-1}$. When this stabilization energy is taken into consideration, the C3 pathway is now favored over that of the C1 pathway in acetone.

A similar situation is found for ECH, only the degree of electrostatic stabilization ($\Delta ES = -1.5\,\text{kcal mol}^{-1}$) is smaller in magnitude. As the C3 mechanism is already preferred in the gas phase, the polar solvent only serves to reinforce this preference in solution.

It should be again noted that the differences between the transitions states for the other solvation energies (e.g., cavitation, etc.) largely cancel one another. For example, the largest absolute differences for the solvation energies were found for the reorganization energies ($\Delta E$), which are only 0.4 and $0.3\,\text{kcal mol}^{-1}$ for EBH and ECH, respectively.

## CONCLUSIONS

*Ab initio* molecular orbital calculations were carried out on EBH and ECH in an attempt to elucidate their reactivity with respect to an archetypal (hard) nucleophile, hydroxide. These systems were examined in both the gas phase and solution under basic conditions.

The gas-phase computations sought to establish the intrinsic reactivity of these substrates to nucleophilic attack; specifically, is the product, glycidol, formed from epihalohydrins through direct displacement of the halide by hydroxide at the acyclic methylene (C1) position or indirectly following attack at cyclic methylene (C3) position of the epoxide ring? In the case of EBH, the direct displacement mechanism was found to be about three times more favorable over the indirect pathway. The indirect displacement mechanism was, however, determined to be nearly 15 times more likely for ECH. In both cases, nucleophilic attack at the methine (C2) position of the epoxide was found to be inconsequential, occurring in less than 1% of the reactions in the gas phase. These results clearly demonstrate that improving the quality of the leaving group ($Cl^-$ to $Br^-$) increases the likelihood of product formation via direct displacement.

When the reaction was modeled in the polar, aprotic solvent acetone, the direct displacement mechanism was effectively shutdown for both epihalohydrins; here, indirect displacement was approximately 200 times more favorable over that of direct displacement. These results can be almost entirely explained by electrostatic arguments; specifically, a sizable dipole moment is produced in the transition state for attack by hydroxide at the C3 position of EBH, which is stabilized by polar solvents such as acetone. As was the case for the gas-phase results, little nucleophilic attack at the C2 position was found to occur in polar solutions. Once again, the appropriate choice of solvent system can bias the reaction mechanism for this system.

The use of computational methods has offered insights into the reactivity of these important chemical systems, which would be difficult to derive solely from experiment. These insights permit the rational choice of leaving groups and solvent systems in the biasing of the reactivity for the epihalohydrins studied. In the final paper in this series, we will examine the gas-phase and solution behavior of epihalohydrins that have been activated by protonation of the epoxide moiety; that is, the reactivity of EBH and ECH under acidic conditions.



DOI: 10.1002/poc

## Acknowledgements

The author would like to express his sincere appreciation to Drs Hyunsoo Han and David Johnson of the Department of Chemistry, the University of Texas at San Antonio for reading and commenting on a draft of this paper.

## REFERENCES

1. For example, an entire issue of a journal was recently devoted to "Cyclopropanes and Related Rings". *Chem. Rev.* 2003; **103**.
2. *Ullmann's Encyclopedia of Industrial Chemistry* (6th edn), Vol. **12**. Wiley-VCH: Weinheim, 2003.
3. Kawamura K, Ohta T, Otani G. *Chem. Pharm. Bull.* 1990; **38**: 2092–2096 (see also toxicological references in 1a).
4. (a) Swern D, Billen GN, Knight HB. *J. Am. Chem. Soc*. 1949; **71**: 1152–1156; (b) Nichols PL, Jr, Ingham JD. *J. Am. Chem. Soc.* 1955; **77**: 6547–6551.
5. McClure DE, Arison BH, Baldwin JJ. *J. Am. Chem. Soc.* 1979; **101**: 3666–3668.
6. Ohishi Y, Nakanishi T. *Chem. Pharm. Bull.* 1983; **31**: 3418–3423.
7. Cawley JJ, Onat E. *J. Phys. Org. Chem.* 1994; **7**: 395–398.
8. Whalen DF. *Tetrahedron Lett.* 1978; **50**: 4973–4976.
9. Politzer P, Laurence PR. *Int. J. Quantum Chem. Biochem. Symp.* 1984; **11**: 155–166.
10. Merrill GN. *J. Phys. Org. Chem.* 2004; **17**: 241–248.
11. (a) Hall GG. *Proc. Roy. Soc. (London)* 1951; **A1951**: 541–552; (b) Roothaan CCJ. *Rev. Mod. Phys.* 1951; **23**: 69–89.
12. (a) Ditchfield R, Hehre WJ, Pople JA. *J. Chem. Phys.* 1971; **54**: 724–728; (b) Hehre WJ, Ditchfield R, Pople JA. *J. Chem. Phys.* 1972; **56**: 2257–2261; (c) Francl MM, Pietro WJ, Hehre WJ, Binkley JS, Gordon MS, DeFrees DJ, Pople JA. *J. Chem. Phys.* 1982; **77**: 3654–3665.
13. Hariharan PC, Pople JA. *Theoret. Chim. Acta* 1973; **28**: 213–222.
14. (a) Clark T, Chandrasekhar J, Spitznagel GW, Schleyer PvR. *J. Comp. Chem.* 1983; **4**: 294–301; (b) Spitznagel GW. *Diplomarbeit*. Erlangen, 1982.
15. McQuarrie DA. *Statistical Mechanics*. University Science Books: Sausalito, CA, 2000.
16. (a) Pople JA, Scott AP, Wong MW, Radom L. *Isr. J. Chem.* 1993; **33**: 345–350; (b) Scott AP, Radom L. *J. Phys. Chem.* 1996; **100**: 16502–16513.
17. Gonzales C, Schlegel HB. *J. Chem. Phys.* 1989; **90**: 2154–2161.
18. (a) Møller C, Plesset MS. *Phys. Rev.* 1934; **46**: 618–622; (b) Binkley JS, Pople JA. *Int. J. Quantum Chem.* 1975; **9**: 229–236; (c) Fletcher GD, Rendell AP, Sherwood P. *Mol. Phys.* 1997; **91**: 431–438.
19. (a) Becke AD. *Phys. Rev.* 1988; **A38**: 3098–3100; (b) Lee C, Yang W, Parr RG. *Phys. Rev.* 1988; **B37**: 785–789; (c) Becke AD. *J. Chem. Phys.* 1993; **98**: 1372–1377.
20. Crawford TD, Schaefer HF. *Rev. Comp. Chem.* 2000; **14**: 33–136.
21. (a) Dunning TH, Jr. *J. Chem. Phys.* 1989; **90**: 1007–1023; (b) Kendall RA, Dunning TH, Jr. *J. Chem. Phys.* 1992; **96**: 6769–6779.
22. Saunders WH, Jr. *J. Phys. Org.* 1994; **7**: 268–271.
23. Tomasi J, Persico M. *Chem. Rev.* 1994; **94**: 2027–2094.
24. (a) Pierotti RA. *Chem. Rev.* 1976; **76**: 717–726; (b) Langlet J, Claverie P, Caillet J, Pullman A. *J. Phys. Chem.* 1988; **92**: 1617–1631.
25. Amovilli C, Mennucci B. *J. Phys. Chem. B.* 1997; **101**: 1051–1057.
26. Mennucci B, Tomasi J. *J. Chem. Phys.* 1997; **106**: 5151–5158.
27. Schmidt MW, Baldridge KK, Boatz JA, Jensen JH, Koseki S, Matsunaga N, Gordon MS, Nguyen KA, Su S, Windus TL, Elbert ST, Montgomery J, Dupuis M. *J. Comp. Chem.* 1993; **14**: 1347–1363.
28. (a) Baker J, Muir M, Andzelm J. *J. Chem. Phys.* 1995; **102**: 2063–2079; (b) Merrill GN, Gronert S, Kass SRJ. *Phys. Chem. A* 1997; **101**: 208–218.



DOI: 10.1002/poc